



Study of Ru (II) Polypyridyl Complex - Synthesis, Characterization, DNA-Binding, Antimicrobial activity and Cytotoxicity

Markandeya Namani¹ and Navaneetha Nambigari^{1,2*}

1. Department of Chemistry, University College of Science, Saifabad, Osmania University, Hyderabad – 500004, Telangana State, INDIA. 2. Department of Chemistry, University College of Science, Osmania University, Tarnaka, Hyderabad – 500007, Telangana State, INDIA.

Abstract - Ruthenium (II) complexes with polypyridyl ligands have been extensively studied as promising functional molecules due to their unique photochemical and photophysical properties as well as cytotoxic properties. Herein, an intercalative ligand, MTPIP [MTPIP = [2-(4-methylthio)phenyl]-1H-imidazo [4,5-f][1,10] phenanthroline] and its mononuclear Ru(II) polypyridyl complex [Ru(A)₂(MTPIP)]⁺² (A=1,10-phenanthroline) have been synthesized and characterized by spectroscopic techniques such as elemental analysis, UV-Vis, IR, ¹H NMR, ¹³C NMR and ESI-Mass. The interaction of the synthesized complex with DNA was studied using Biophysical Methods (Absorption, emission and viscosity methods). The study reveals that the Ru(II) polypyridyl complex binds to DNA preponderantly by intercalation. The complex showed absorption, hyperchromism in its UV-Vis spectrum with DNA. The binding constant K_b from UV-Vis absorption studies was 2.5 × 10⁵ and Stern-Volmer quenching constant (K_{sv}) from fluorescence studies was 5.5 × 10³. Finally viscosity measurements revealed that the binding of the complex with CT-DNA is groove binding. In photo cleavage studies the complexes successfully cleaved the pBR 322 DNA. Ru(II) polypyridyl complex was examined for their antimicrobial activity. This was assessed against antibacterial (Staphylococcus, Bacillus, E. Coli & Klebsiella) and anti-fungal (Candida & Aspergillus). The cytotoxic activity of these Ru(II) complex was carried by MTT assay with MCF-7 cell lines. MTT assay of the complex reveals good anticancer activity against MCF-7 cell line as IC₅₀ = 14.54 ± 0.19 μg/ml indicating correlation with DNA binding affinity.

Keywords: Polypyridyl, Biophysical, DNA binding, Photo cleavage, Cytotoxicity, Antimicrobial activity

1. INTRODUCTION

Bio inorganic chemistry is an emerging field of biomedical research and health care since twenty - first century [1-2]. Bacterial infections are a significant global health concern due to the enhanced multi-drug resistant pathogens [3-5]. The great success in the clinical treatment of human malignancies has stimulated research in the area of inorganic anti-tumor agents. [6] Nucleotides are essential components of DNA and RNA which play important roles in the storage and transfer of genetic information and protein biosynthesis in living organisms [7-9].

According to the world health organization (WHO), and Indian council of medical researcher's latest report on anti-microbial resistant research and surveillance, mutation in micro-organisms result in the growing. Antimicrobial resistance (AMR); as a result leave antibiotics ineffective and infections to persist [10, 11]. Luminescent signaling systems that respond to external stimuli which are important for the design of molecular switches and molecular machines have received much attention recently [12, 13] proton-induced luminescent switches are especially appealing for the measurement of P^H and PCO₂ in biological, chemical and environmental monitoring. Various luminescent dyes have been explored for the development of optical P^H sensors, including fluorescein, naphthalene, Carrole and coumarin derivatives [14, 15]. Investigations of luminescent transition metal complexes have attracted less attention and their great potential as P^H sensors has not fully been explored [16, 17]. Imidazole-containing ligands are poor π acceptors and good π donors compared with pyridine-pyrazine and pyrimidine-containing ligands. Further-more imidazole containing ligands possess ionizable N-H protons which can perturb the electronic properties of their metal complex through protonation and deprotonation. Although some Ru (II) polypyridyl complexes containing imidazole units have been prepared, in most cases, these complexes are non-emissive or weakly emissive associated with deprotonation processes [18]; only those with imidazole units un-coordinated to the Ru (II) centers are good emitters. To the best of our knowledge, only a few mono and di nuclear Ru (II) polypyridyl complex of this kind

have been reported platinum containing drugs, which are widely used in cancer treatment^[19,20]. The great success in the clinical treatment of human malignancies has stimulated research in the area of inorganic antitumor agents^[21]. However, their use is tremendously impeded by severe toxicity and development of resistance during the treatment^[22, 23]. In order to overcome these disadvantages, contemporary strategies in the development of novel metallo drugs focused more and more on the use of transition metal complexes containing improved organic ligands^[24 - 26]. Ruthenium has one metal that has been targeted as a replacement for platinum-based drugs due to its generally reduced host toxicity and interesting redox properties.^[27 - 29] Ruthenium (II/III) complexes have unique feature they are six coordinated in both oxidation states low spin and their substitution reaction rates are smaller than of corresponding first row complexes^[30]

Molecular modeling of transition metal includes the prediction, interpretation of structures and also the correlation between structures and properties (thermodynamics, reactivity's, electronics). Empirical force field calculation may yield accurate structural predictions of transition metal complexes^[31].

Ruthenium (II) mimics iron, which is an important feature for biological aspects such as it can take advantage of the body's ability to efficiently transport and uptake of iron. This effect contributes to the lower toxicity that is associated to the ruthenium drugs in comparison to platinum it is important to note that the ruthenium is not necessarily replacing the iron within these proteins, but that they are transported concurrently^[32]. Eukaryotic and bacterial DNA exhibit comparable features, restricting the feasibility of selective targeting of bacterial DNA. It is believed that metal-based drugs have atypical system of action against cancer and bacterial cells. The toxicity, in addition, to severe issues indicates, the requirement for improved drug treatments. DNA, the carrier of hereditary details, has been recognized as the primary target for a variety of antimicrobial drugs due to their capability to interfere with DNA transcription and replication, which are major steps of cell growth and division^[33].

In the current study, the synthesis of ligand MTPIP [2-(4-methylthio) phenyl]-1H-imidazo [4,5-f][1,10] phenanthroline and its metal complex and characterization of the complex was achieved by IR, UV, ¹H NMR, ¹³C NMR, Mass and elemental analysis. The binding study of CT-DNA to this complex was investigated using UV-Visible absorption titration, Fluorescence emission and Viscosity experiment. The complex exhibited cleavage of plasmid pBR322 DNA effectively. The complex was screened for their antimicrobial and cytotoxic activity.

2. EXPERIMENTAL

Except where otherwise noted, all analytical grade reagents and solvents were used exactly as they were supplied. The following substances were purchased from Merck: 1,10-phenanthroline monohydrate (phen), 2,2'-bipyridine (bpy) and 4,4'-dimethyl-2,2'-bipyridine (dmb). Super coiled PBR 322 plasmid DNA (Stored at 20°C) and calf thymus DNA (CT-DNA) were obtained from Fermentas Life Science and Aldrich, respectively, and used in their original forms. From Genei, agarose gel was purchased. All studies used 18.2mX ultrapure Milli-Q water, tris (hydroxymethyl) amino methane, tri-HCl buffer (5m.mol. Tris HCl, 50 mM NaCl, pH 7.2), the binding affinity of the metal complex for CT-DNA was estimated. At absorbance of 260 and 280 nm and a concentration of DNA per nucleotide at a molar extinction of 6600 cm⁻¹ protein-free DNA could be seen using spectrophotometer. Stock solutions of metal complexes were prepared in the DMSO solvent and kept at 40°C, used in less than 5 days. All the stock solution were diluted further for required concentration in buffer.

The Shimadzu UV-2600 spectrophotometer was used to record the UV-Vis spectra. The Cary Eclipse instrument serial number (MY12400004) Spectrofluorometer was used to record the luminescence spectral data needed to calculate the binding constants. Using KBr disks, IR spectra were recorded using a PerkinElmer 1605 Fourier transform IR Spectrometer. With tetramethylsilane serving as the internal standard and dimethyl-d₆ sulfoxide (DMSO-d₆) serving as the solvent, ¹H and ¹³C NMR spectra were captured using a Bruker 400-MHz spectrometer. The PerkinElmer 240 elemental analyzer was used to do elemental microanalysis on the element C, H and N. A Quattro LC triple quadrupole mass spectrometer equipped with the mass Lynx software (Micro mass, Manchester, UK) was used to record the mass spectra.

2.1. Synthesis, characterization of ligand (MTPIP) and its Ru (II) complex

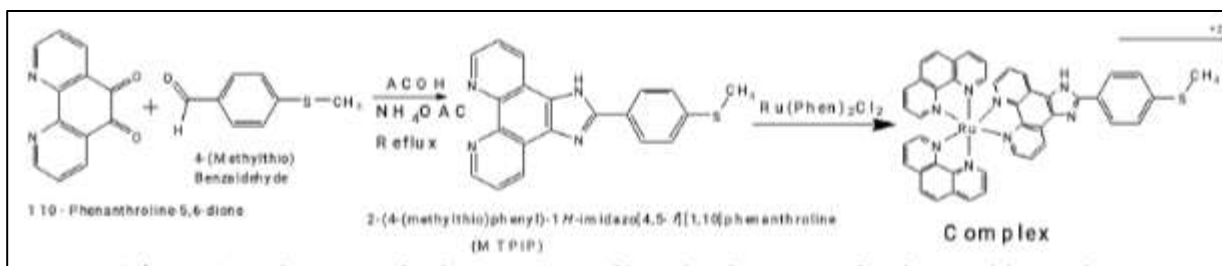
The 1, 10-phenanthroline-5,6-dione and [Ru(A)₂Cl₂], Starting materials were synthesized according to the standard procedure where A= Phen^[34, 35]. Synthetic route for ligand and complex is shown in Scheme-1.

2.1.1. Synthesis of MTPIP - [2-(4-methylthio) phenyl]-1H -Imidazole [4,5-f] [1,10] phenanthroline](L)

The ligand was synthesized using phen dione (0.25gm, 1.189 mmol), 4- (Methylthio) Benzaldehyde (0.18 gm, 1.18 mmol) and ammonium acetate (2.334 gm, 30 mmol) were dissolved in glacial acetic acid (15ml) and then refluxed for 5 hour. The result was a distinct brick-red colour solution, cooled to room temperature and transferred to distilled water, where the con NH₃ was added drop wise to produce an orange-yellow precipitate that was collected. Washed with H₂O and dried. The crude product recrystallized with C₂H₅N.H₂O and dried. Yield: 68.4%.

Analytical data:

C₂₀H₁₄N₄S: Calcd (%): C: 70.1; H: 4.09, N: 16.3; Found (%): C : 70.3 ; H : 4.1 ; N : 16.2 ES⁺ - MS Calc : 342; Found : 343.4 ; ¹H NMR (DMSO-d₆, 400 MHz): δ ppm; δ 9.02(d,2H), δ 8.94(d,2H), δ 8.24 (d,2H) δ 13.74(s,1H), δ 7.81 (d,2H), δ 7.46(d,2H), δ 2.57(s,3H); ¹³C [¹H] NMR(100 ,MHz,DMSO-d₆,ppm): 150.92, 148.05, 143.91, 140.62, 131.57, 130.13, 127.10, 126.99, 126.24, 123.65, 122.04, 14.78 ; IR (KBr, cm⁻¹): 3454 (ν, N-H), 2924 (ν, C-H), 1741 (ν, C-N), 1092 (ν, C-S-C), 694 (ν, C-S)



Scheme-1: Synthetic route for the preparation of ligand and structure of Ruthenium (II) Complex.

2.1.2. Synthesis of [Ru(Phen)₂(MTPIP)] (ClO₄)₂H₂O

A mixture of *cis* [Ru(Phen)₂Cl₂] 2H₂O (0.5mM,0.284g) and MTPIP ligand (0.5 mM,0.171 g) in ethanol (15ml) refluxed for 14 h at 120°C under a purge of N₂ gas. The resulting light purple color solution was cooled to room temperature before adding an equivalent amount of saturated aqueous NaClO₄ solution under vigorous stirring. The red solution under was collected and cleaned with modest amount of diethyl ether, ethanol and water, before being vacuum dried (Yield 62.3%) (Scheme 1).

Analytical date for RuC₄₄H₃₄N₈S : Calcd (%): C : 56.3 , H : 3.6 , N : 11.9; Found (%): C : 56.4 , H : 3.5 , N : 12.0; ES⁺-MS calcd : 937 Found: 937.1 ;¹H NMR (DMSO-d₆,400 MHz): δppm: δ 8.96 (d,6H), δ 9.06(t,6H) δ8.39 (s,4H) δ8.25(d,2H), δ 8.09 (d,2H) δ13.8 (s, NH) δ7.77 (s,2H) δ 7.53(d,2H) δ 2.507(s,3H); ¹³C [¹H] NMR (100 MHz,DMSO,D₆,ppm): 158.1 ,149.9 , 148.6 ,139.2,139.4 ,136.4 ,129.2 ,127.6 ,125.2 ,121.5, 14.8 ; IR(KBr,CM⁻¹): 3575 (ν,N-H) ,2923 (ν,C-H) ,1740 (ν,C-N) 1089 (ν,C-S-C) ,623 (ν, Ru-N).

2.2. DNA binding studies

The techniques employed in our procedure to determine the binding affinity for the Ruthenium (II) polypyridyl complex are the main topics of this section which were discussed in our protocols [36 - 38].

2.2.1. Electronic absorption studies

The tries (hydroxymethyl)-amino methane (Tries,5mM),sodium chloride (50mM),and hydrochloric acid were added to double - distilled water to create the proper P^H balance for the experiments comprising the interaction of the ruthenium(II) Complexes with CT-DNA. The ratio of UV absorbance from a solution of CT-DNA in the buffer was roughly 1.9 at 260 and 280 nm, demonstrating that the DNA was adequately free of protein. Using the molar extinction coefficient value of 6600 dm³ mol⁻¹ cm⁻¹ at 260 nm, absorption spectroscopy was used to calculate the DNA concentration per nucleotide. The nucleotide concentration was varied from 10 to 100 μm while the complex concentration was kept constant (20 μm) for the electronic absorption titration studies. Equal quantities of DNA were used to measure the absorption spectra.

$$[DNA]/(\epsilon_a - \epsilon_f) = [DNA]/(\epsilon_b - \epsilon_f) + 1/K_b (\epsilon_b - \epsilon_f) \quad \dots (1)$$

The apparent absorption coefficient ϵ_a , ϵ_f and ϵ_b equate to $A_{obsd}/[complex]$, the extinction coefficient of the compound while it is free, and the extinction coefficient of the compound when it is fully bound to DNA, respectively, where [DNA] is the concentration of DNA in base pairs . K_b is determined by plotting $[DNA]/(\epsilon_a - \epsilon_f)$ versus [DNA] and K_b calculated using the slope to intercept ratio as shown in equation 1.

2.2.2. Fluorescence emission studies

The previously described approach was used to perform the emission titrations. In these titrations, the metal complex concentration was maintained at optimal level while raising the DNA concentration to record the spectra; these emission values fell between 550 and 750 nm. The formula used to determine the binding constant is shown in equation 2.

$$C_b = C_t [(F - F_0) / (F_{max} - F_0)] \quad \dots (2)$$

Where C_t is the total complex concentration, is the observed fluorescence emission intensity at a given DNA concentration, F_0 the emission intensity in the absence of DNA, and F_{max} is the time when the complex is maximally bound to DNA. A graph was created between the r/c_f vs r , binding constant, where r is the $C_b/[DNA]$ and C_f is the concentration of the free complex, using the Scatchard equation 2 to compute the binding constant.

2.2.3. Viscosity experiment

Utilizing an Ostwald's viscometer kept in a thermostatic bath at a constant temperature of $29 \pm 0.1^\circ\text{C}$, viscosity measurements were taken. Each sample's flow time was measured three times using a digital stopwatch, and the average flow time was computed. Data are displayed as $(\eta/\eta_0)^{1/3}$ vs binding ratio [39], where η is the DNA's viscosity when the complex is present and η_0 is the DNA's viscosity when CT-DNA is used alone. The measured flow time of DNA-containing solutions (t) was used to determine the viscosity values, which were then adjusted for the observed flow time of the buffer alone (t_0)

2.2.4. Quenching studies

The Tris-HCl buffer solution ($p^H=7.5$) was employed in the fluorescence experiments. Different concentrations of the complexes (1,2,3,and 4) were added to an ethidium bromide and CT-DNA solution to allow for reaction. The concentrations of the complexes was kept between 10 and 100 μM , whereas ethidium bromide and CT-DNA were kept at 130 and 140 μM respectively. Ethidium bromide's emission range was kept between 560 and 760 nm, and its emission spectra was observed at 520 nm. By using the Stern-Volmer equation: $I_0/I=1+K_{SV}r$, where I and I_0 stand for fluorescence intensities in the presence and absence of complexes, respectively, and K_{SV} linear Stern-Volmer quenching constant based on the ratio of r_{EB} (the ratio of the bound concentration of EB to the concentration of DNA) and total concentration of the complex to that of DNA, is r thus the spectra were examined [40].

2.2.5 DNA cleavage experiment

By using the agarose gel electrophoresis method, the metal complexes capacity to cleave DNA through photolytic investigation was calculated. In this test, metal complexes were applied to super coiled pBR322 DNA at several quantities, and then DNA was diluted with Tris-HCl buffer at $p^H7.2$. The pretreatment DNA-sample system was mixed with bromophenol blue (2L) and then incubated for a further two hours at 37 °C. The samples were then loaded onto the wells of a 1% agarose gel that was set in a tray containing TAE buffer (p^H 8.0) for 45 minutes at 70 V. Before electrophoresis, the gel was treated with ethidium bromide on a BIO-RAD Gel documentation system, bands were seen under an ultraviolet (UV) transilluminator [41].

2.3. Antimicrobial activity

Antimicrobial studies were performed by using pour plate method. The complex was tested for their antimicrobial activity against Staphylococcus Aureus, Bacillus Subtilis, E.Coli, Klebsiella Pneumonia, Candida and Aspergillus. Four different concentrations (25 μL , 50 μL , 75 μL & 100 μL) in DMSO was used for testing spore germination of each fungus. In this method 1% of active bacterial and antibiotic (Streptomycin/Chloramphenicol) cultures were mixed into autoclaved agar media just before solidifying temperature and poured into the petri plates. After the plates were solidified, wells were made using sterile well borer and samples were loaded 100 μL each into the wells respectively. Plates were incubated at 37°C for 18-24 hours in a bacterial incubator and at 25°C for 96 hours in fungal incubator. They were the observed and diameters of the inhibition zone (in mm) were measured and tabulated. These results were compared with standard antibacterial drug streptomycin (5 $\mu\text{g/ml}$) and antifungal agents Fluconazole (5 $\mu\text{g/ml}$) for candida, Mancozeb Wp 75 (5 $\mu\text{g/ml}$) for aspergillus at same concentration.

2.4. Cytotoxicity

The cells were seeded in a 96-well flat bottom micro plate and maintained at 37° C in 95% humidity and 5% CO₂ overnight. Different concentration (100, 50, 25, 12.5, 6.25, 3.125 $\mu\text{g/ml}$) of sample were treated. The cells were incubated for another 48 hours. The wells were washed twice with PBS and 20 μl of the MTT staining solution was added to each well and the plate was incubated at 37°C. After 4h, 100 μL of DMSO was added dissolve to each well to dissolve the formazan crystals, and absorbance was recorded with a 570 nm using micro plate reader [42].

Formula: Surviving cells (%) = Mean OD of test compound / Mean OD of negative control x 100

Using graph pad Prism version 5.1, we calculate the IC₅₀ of compounds.

3. RESULTS AND DISCUSSION

3.1. Synthesis and Characterization

Synthesis of the novel complex is confirmed by CHN analysis, mass, ¹H NMR, ¹³C NMR, FTIR & Absorption spectrum. IR spectrum shown bands at 3454(ν ,N-H), 2924(ν ,C-H), 1741(ν ,C-N), 1092(ν ,C-S-C) after complex formation the bands further shifted to 3575(ν ,N-H), 2923 (ν ,C-H), 1740(ν ,C-N), 1089 cm^{-1} (ν ,C-S-C). The appearance of new band at 623 cm^{-1} in the IR spectra of complex which is due to the formation of metal- nitrogen bond (ν , Ru-N) confirm the complex formation (Figure 1, 2). In the ¹H NMR spectra of the complex, the peaks due to different protons of ligand shifted downfield in complex as compared to the ligand (MTPIP) ¹H NMR spectra show the ligand characteristic aliphatic peak at 2.508 ppm, these proton were shifted to around 2.507ppm after complex formation (Figure 3, 4). In the complex, the N-H proton appeared around 14 ppm, ¹³C spectra of the complexes show shift in the complexes show shift in the chemical shift values compared to ligand, confirming the complex formation (Figure 5, 6). M/Z values from the mass correlates with theoretical value (Figure 7,8). The MLCT band in absorption spectrum for the complex appeared at 420 nm which is not shown by ligand, confirming complex formation (Figure 9, Table 1).

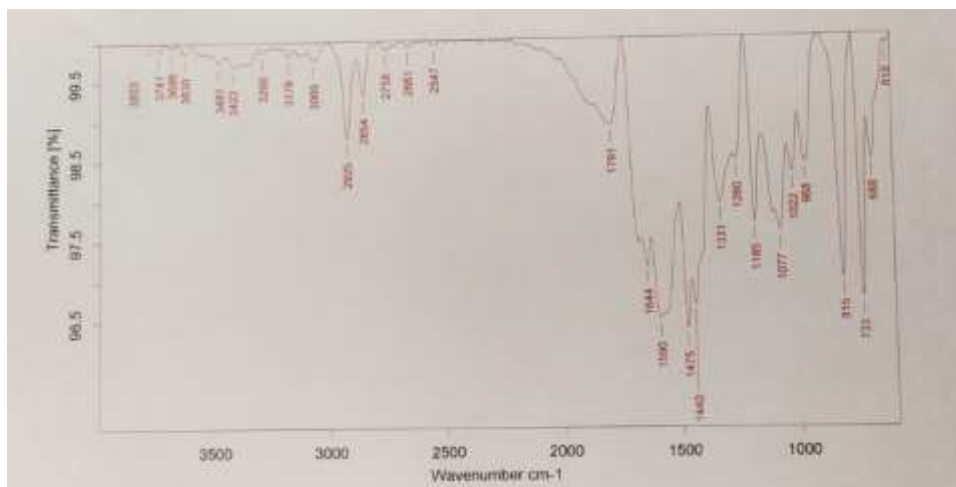


Fig.1. IR Spectra of intercalator Ligand, MTPIP.

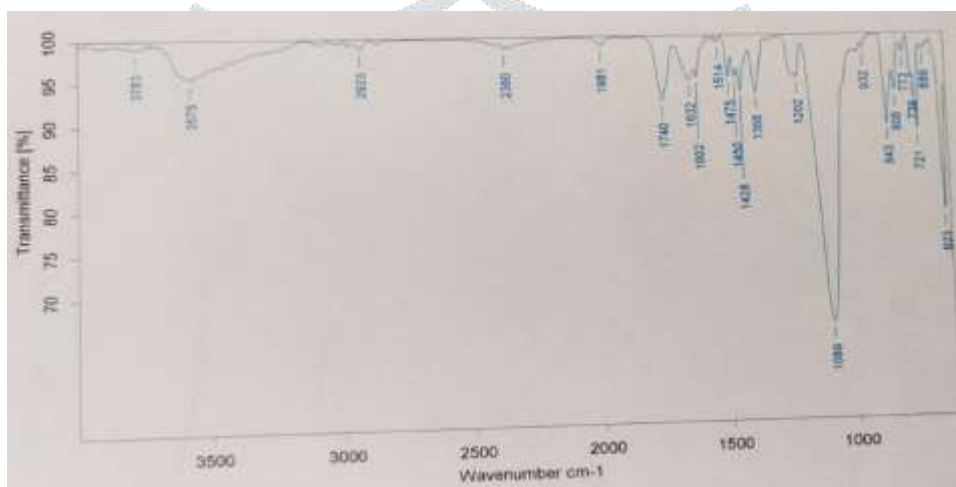


Fig.2. IR Spectra of [Ru(phen)₂(MTPIP)]⁺² Complex

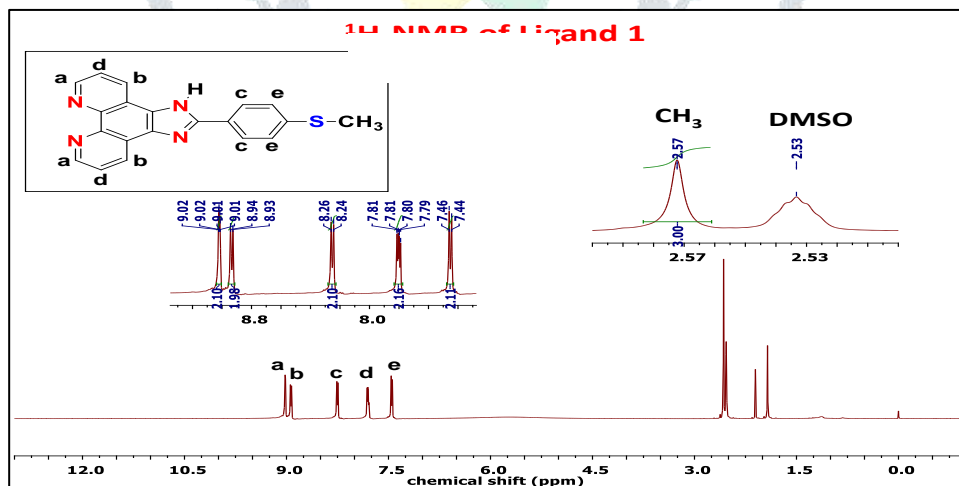


Fig.3. ¹H NMR Spectra of Intercalator, Ligand MTPIP

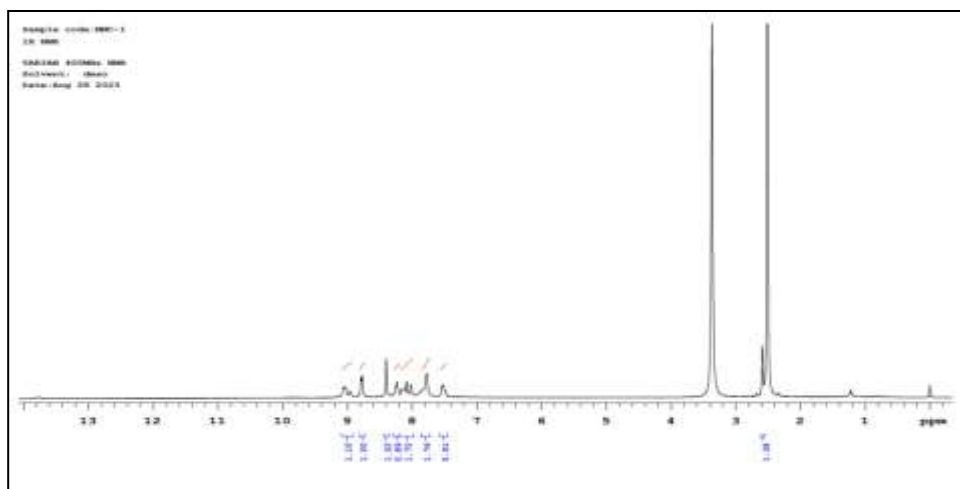


Fig.4. ¹H NMR Spectra of [Ru(phen)₂(MTPIP)]⁺² Complex

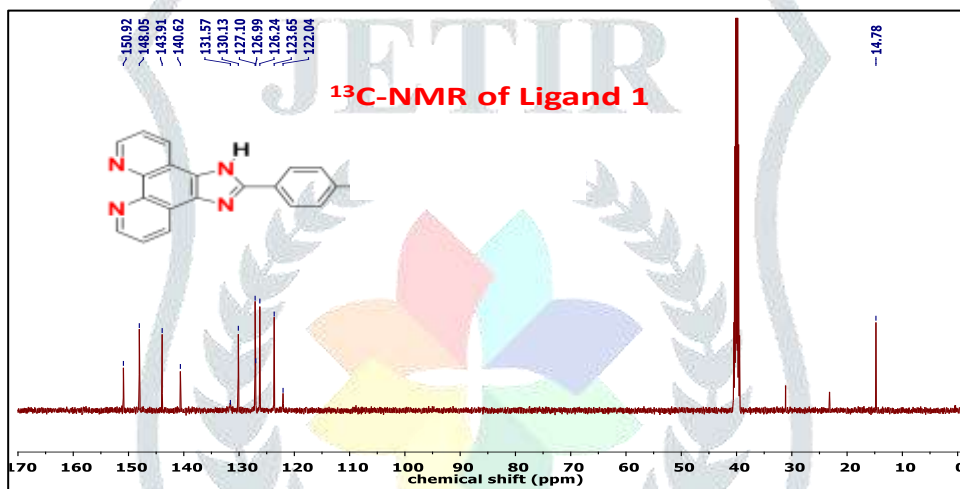


Fig.5. ¹³C NMR Spectra of Intercalator ,Ligand MTPIP

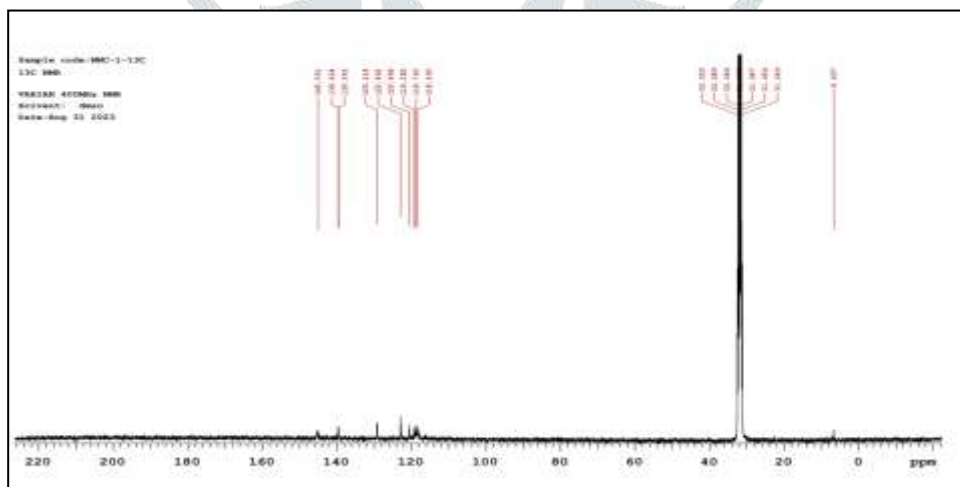


Fig.6. ¹³C NMR Spectra of [Ru(phen)₂(MTPIP)]⁺² Complex

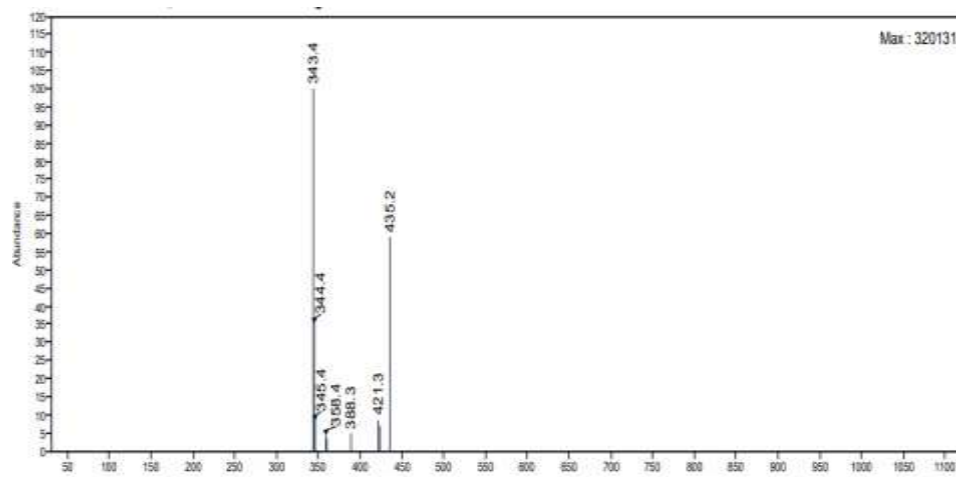


Fig.7. Mass Spectra of Intercalator, Ligand MTPIP

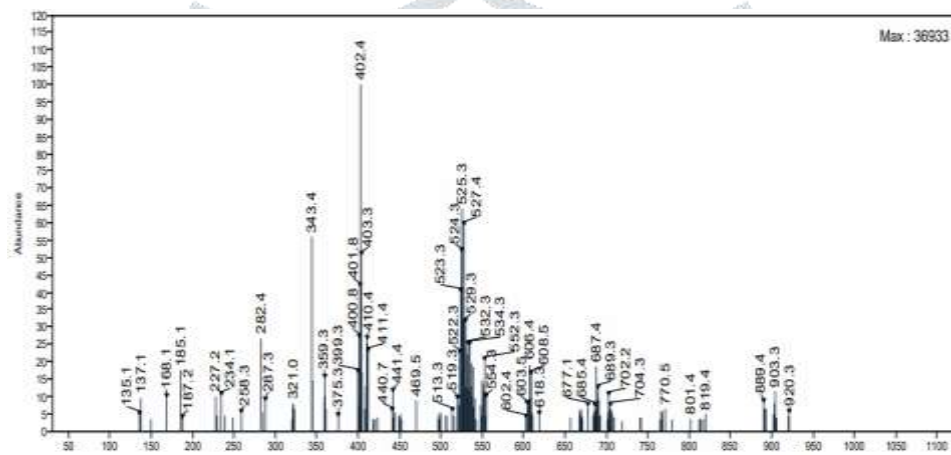


Fig.8. Mass Spectra of $[\text{Ru}(\text{phen})_2(\text{MTPIP})]^{+2}$ Complex

3.2. DNA binding studies

3.2.1. UV-Visible absorption studies

The UV Visible spectra of complex show characteristic MLCT transition in the visible region. Binding affinity of metal complexes to CT-DNA can be characterized by hypochromism and bathochromism in MLCT band. Electronic absorption titration was performed in the presence and absence of DNA was shown in the Figure 9.

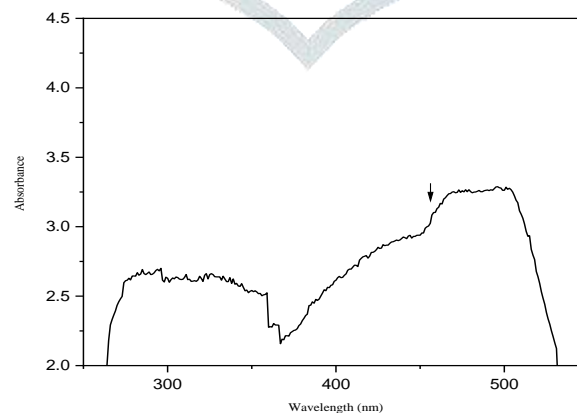


Fig.9. Electronic absorption Spectra of Meta Complex

Table.1. Electronic Spectral data of Metal Complex

Complex	Absorption region, λ_{max}	Band assigned
[Ru(phen) ₂ (MTPIP)] ⁺²	275 455	$\pi \rightarrow \pi^*$ (MLCT)

The metal complex concentration kept constant, to this increased concentrations of CT-DNA added. By the addition of increase amounts of DNA decrease in the absorption observed in the MLCT band region at 420 nm respectively. Hypochromic shift of 19.03% and bathochromism of 4nm of complexes. Hypochromism shift result due to strong p-p stacking interaction between intercalated aromatic chromophore of metal complex and base pair units of DNA. Bathochromism result due to coupling of antibonding P orbital's of intercalated metal complex with bonding P orbitals of DNA base pair which leads to a decrease in P-P* transition energy. π - π interaction between the metal complex aromatic chromophore and the DNA base pair units leads hypochromism. The interaction of anti-bonding orbitals (π) of intercalated metal complex with bonding (π) orbitals of DNA leads to bathochromism. Figure 10 show the UV-Visible absorption spectra of complex in the presence (lower) and in the absence (Top) of CT-DNA in Tris-HCl buffer. The titration of the metal complex solution (constant 10 μ m of 0.001 M concentration) in Tris-HCl buffer in the cuvette, and 0-120 μ L of DNA (stock concentration = 0.617×10^{-4} M) is added to the buffer solution. The intrinsic binding constant (K_b) calculated by linear fit of the changes in the absorbance of the complex at 420 nm by using equation.1. The binding constant values for the complexes 2.5×10^5 respectively (table.2). The complex has shown good binding result, owing to more planarity of ancillary ligand phen.

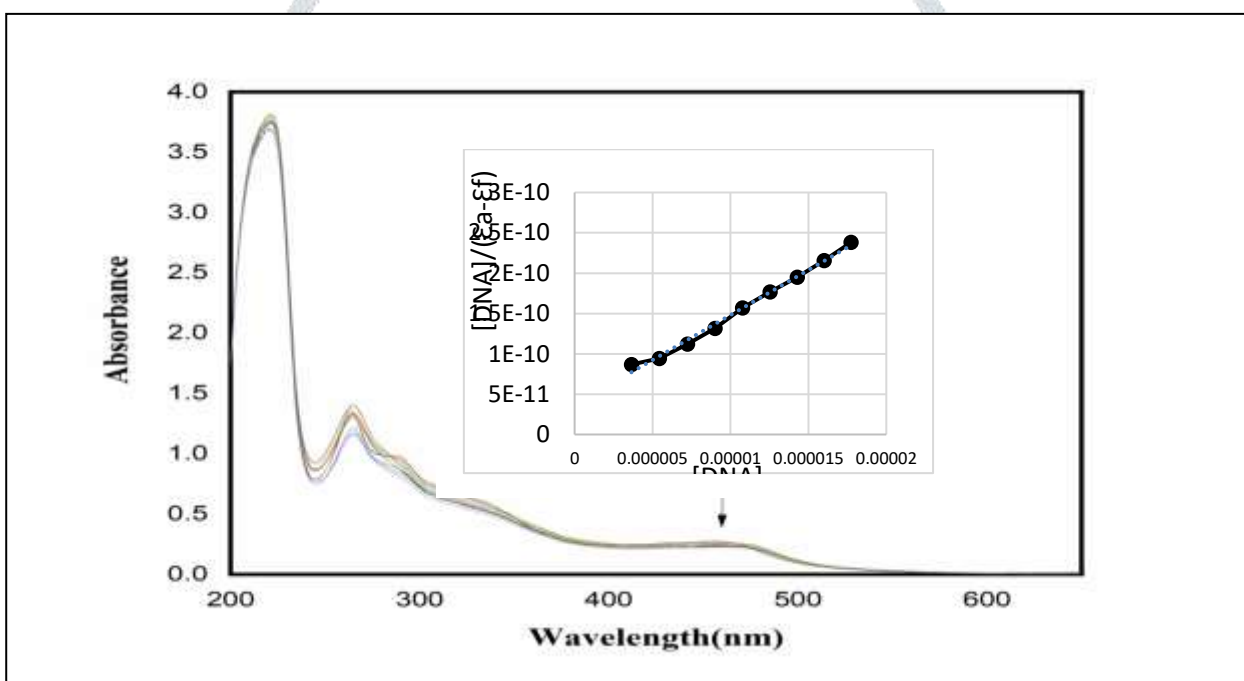


Fig.10. Changes upon increase of DNA concentration is represented with the arrows, inserted a Plot by taking $[DNA]/(\epsilon_a - \epsilon_f)$ Vs $[DNA]$ for the titration of DNA with Ru(II) polypyridyl Complex which gives intrinsic binding constant (K_b).

3.2.2. Fluorescence emission studies

The binding strength of metal complex to CT- DNA further assessed by Fluorescence emission titrations. The complex excited at 420 nm then strong emission observed at 607 nm band region respectively. While increasing the concentration of CT- DNA change in the emission intensity of the complex is shown in the Figure 11. The complex emission intensities gradually rise with increasing DNA concentration until they reach a steady level.

The modified scatchard equation used for the calculation of intrinsic binding constant (K_b) from emission data. Binding constants (K_b) were obtained from scatchard equation used for the calculation of intrinsic binding constant (K_b) from emission data. Binding constants (K_b) were obtained from scatchard plots where r/c_f Vs r is plotted. Where c_f is free ligand concentration, r is the binding ratio $C_b / [DNA]$. The K_b values for complex is 4.1×10^5 . The values obtained from absorption and emission titration were in accordance with each other.

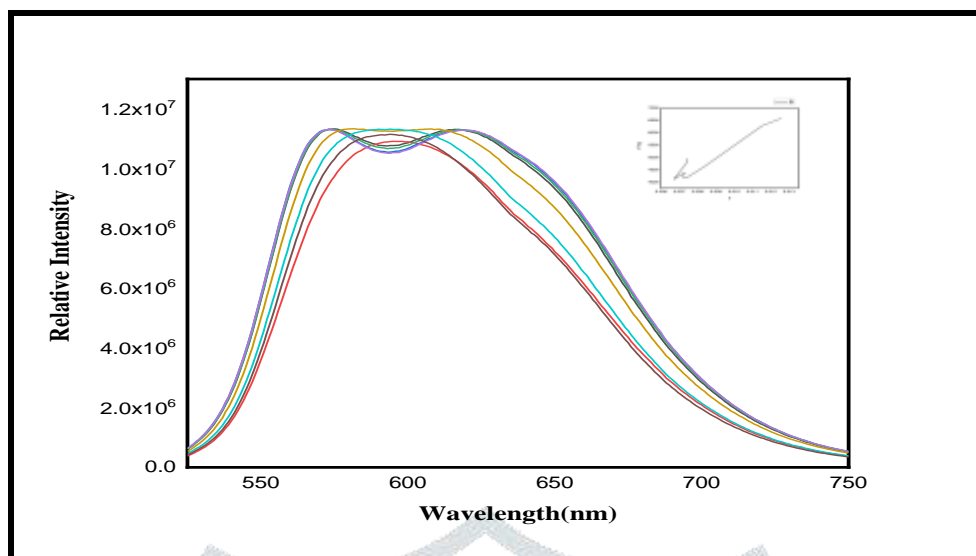


Fig.11. The Ruthenium (II) complex emission spectra in Tris-HCl buffer. Upon the addition of CT-DNA; the arrow shows the intensity change by increasing DNA concentration. Inset: Scatchard plot of the complexes, from which Binding constant (K_b) calculated.

Table 2. Absorption, Emission, and Quenching Binding Constants of Ruthenium (II) complex with CT-DNA.

Complex	K_b (M^{-1}) (Absorption)	K_b (M^{-1}) (Emission)	K_{sv} value
$[Ru(Phen)_2(MTPIP)]^{+2}$	2.5×10^5	4.1×10^5	5.5×10^3

3.2.3. Quenching studies

It has been shown that DNA groove binders and intercalator can both diminish the fluorescence intensity. However, the reduction caused by groove binders is only minor, whereas the replacement of ethidium bromide (EB) by intercalator can result in a considerable reduction in intensity. Further fluorescence investigations using the quenching method were used to determine the intercalative mode of complex binding to CT-DNA. When EB intercalate with DNA, there is a dramatic increase in emission intensity, representing the way that EB interacts with DNA base pair units. In the current study, the solution of ethidium bromide [40 μM] and CT-DNA [130 μM] and increased amount of complex [10-100 μM] were added. As a result, the intensity of the fluorescence emission was reduced which was shown Figure 12. The outcome was approximated using the Stern-Volmer equation and indicates that complexes may bind to CT-DNA and replace EB from DNA. This indicates the intercalation of the complexes to CT-DNA. Stern-Volmer equation used to calculate the results. K_{sv} value is obtained from the linear fit plot of I_0/I versus $[complex]/[DNA]$ is $5.5 \times 10^3 M^{-1}$ obtained.

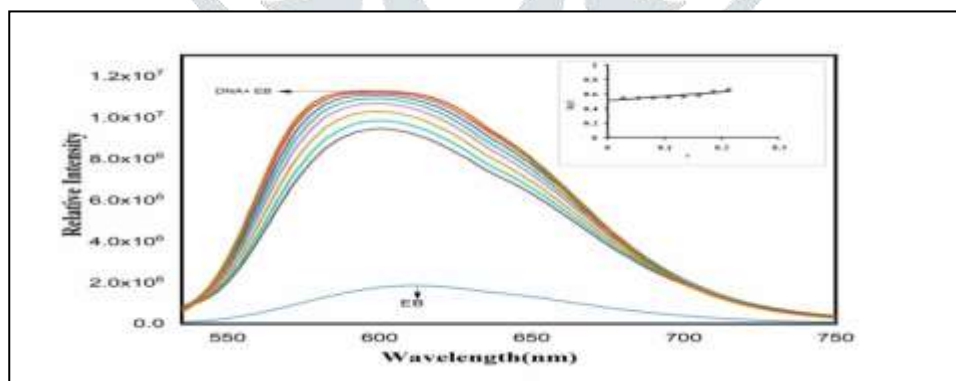


Fig.12. Fluorescence quenching studies of DNA-EB complex (DNA[130mM] & EB[40mM]) system, with the addition of complex arrow shows the decreasing emission intensity by increasing the concentration of complex[10 – 100 mM], Inset : I_0/I versus r .

3.2.4. Viscosity studies

Viscosity studies conducted to find out the mode of binding of the metal complex to CT-DNA. Hydrodynamic experiments are crucial to understand the length change and stiffening of the rod-like DNA by inserting ligand between neighboring base pairs of DNA in solution in the absence of crystallographic data. Intercalating ligands, intercalates in between the base pairs of DNA which lengthens the double helix and by increases the viscosity of DNA solution. Classical intercalation binding model shows increased

viscosity of DNA by lengthening of DNA helix due to the separation of double helix to accommodate the ligand in between the base pairs [43]. The best example for classical intercalation binding mode was observed in EtBr. In this study, increased concentrations of complexes were added to the CT-DNA resulting in an extension in the DNA length there by increased viscosity observed.

Further on comparison with EtBr an intercalating ligand as shown in the Figure 13, the results of the complex binding in between the base pairs of DNA which support intercalation binding mode. The results are strongly supported by observation from electronic spectroscopy and fluorescence emission.

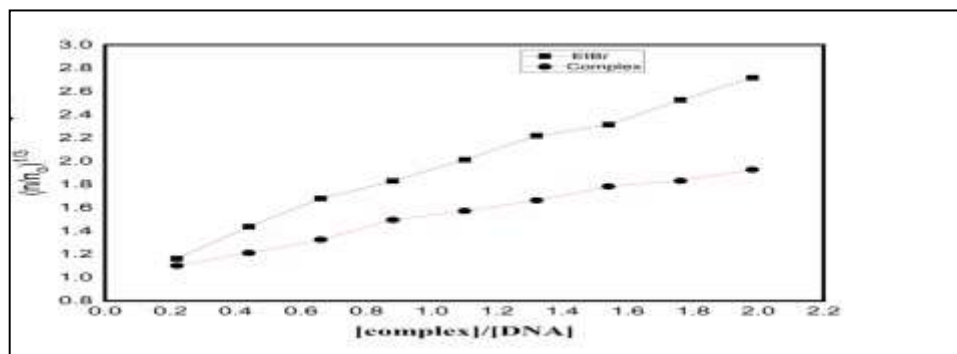


Fig 13. Viscosity study of complex in Tris-HCl buffer with increasing amounts of complex and Et Br on the relative viscosity of CT –DNA at room temperature

3.2.5. Photo cleavage

Using pBR322 DNA, nuclear activity of the Ru (II) Complex was measured using agarose gel electrophoresis. When the super coiled shape is intact, migration is seen in form I, if nicking, or scission on a single strand, happens, then a slower-moving, open circular form (form II) will result from the super coiled form relaxing. When both threads are split, a linear form known as form III moves, this form is migrates in between I and II. Photo cleavage experiment was performed by taking pBr322 which was incubated along with the complex (20 μM) and irradiated for 60 min at 365 nm under UV light continuously. When the metal complex was absent no signs of DNA cleavage shown in lane 1. Once the amount of Ru(II) complex was added, the equivalent of form I progressively dropped, while the quantity of type II enhanced, as Figure 14 illustrates.

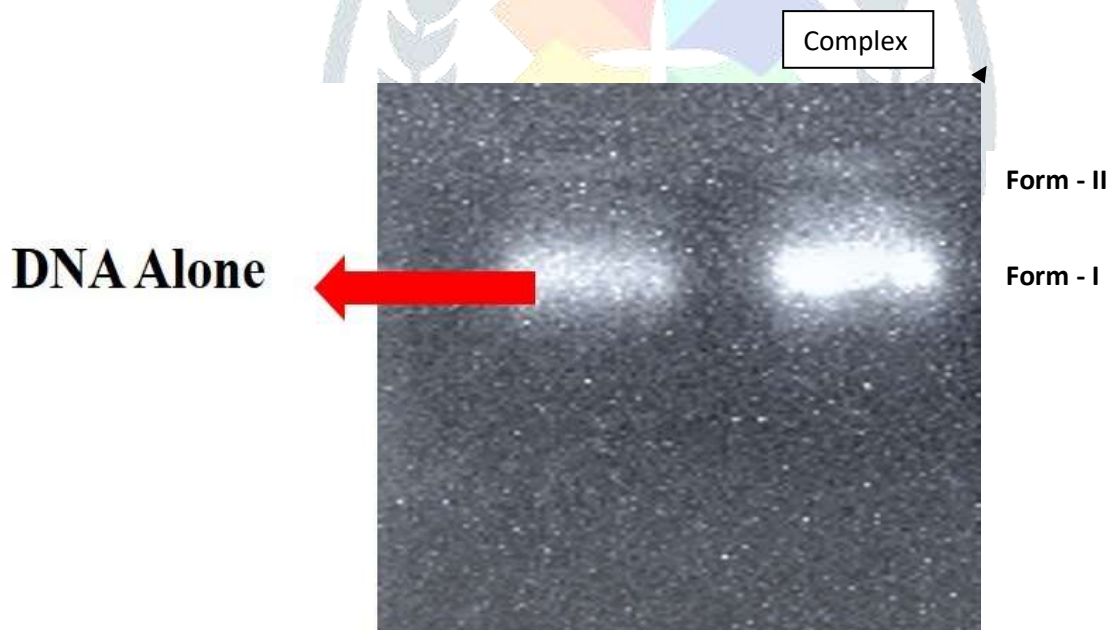


Fig.14. Photo activated cleavage $[\text{Ru}(\text{phen})_2(\text{MTPIP})]^{+2}$ complex with the Concentration range of 20 μM

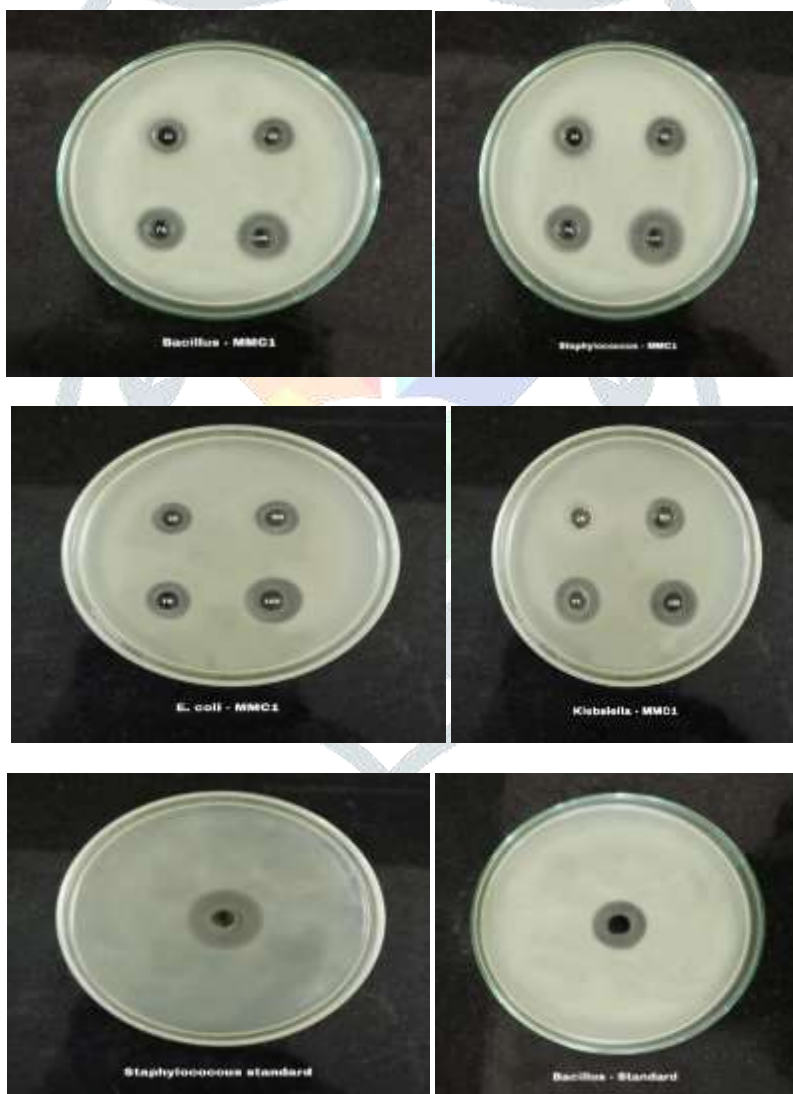
3.3. Antimicrobial Activity:

The antibacterial activity data (Table 3) indicate that the complex show a high activity against both staphylococcus aureus (gram positive bacteria) at 25μL of sample concentration and Klebsiella (gram negative bacteria) at 50μL of sample concentration as shown in Figure 15. The antifungal activity data (table 3) indicate that the complex show an appreciable activity against Candida at 50μL of sample concentration and are expressed as inhibition zone diameter (in mm) versus standard as shown in Figure 16.

Table.3.Antimicrobial activity of [Ru(phen)₂(MTPIP)]⁺² complex.

	Minimum Inhibitory Concentration-MIC (*mm)												MIC of sample (µL)
	Gram positive bacteria				Gram negative bacteria				Candida		Aspergillus		
	Staphylo coccus		Bacillus		E.Coli		Klebsiella						
Complex	75 µL	100 µL	75 µL	100 µL	75 µL	100µL	75µL	100 µL	75µL	100 µL	75 µL	100 µL	25µL
	12 mm	14mm	10 mm	12 mm	09 mm	12 mm					08 mm	12 mm	
							12 mm	14 mm	12 mm	14 mm			50µL
standard	16mm		14mm		12mm		12mm		12mm		12mm		

*The zone of inhibition in mm.



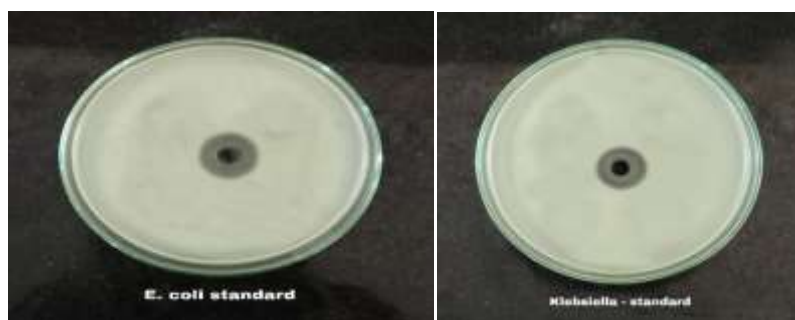


Fig.15. Antibacterial activity of $[\text{Ru}(\text{phen})_2(\text{MTPIP})]^{+2}$ Complex

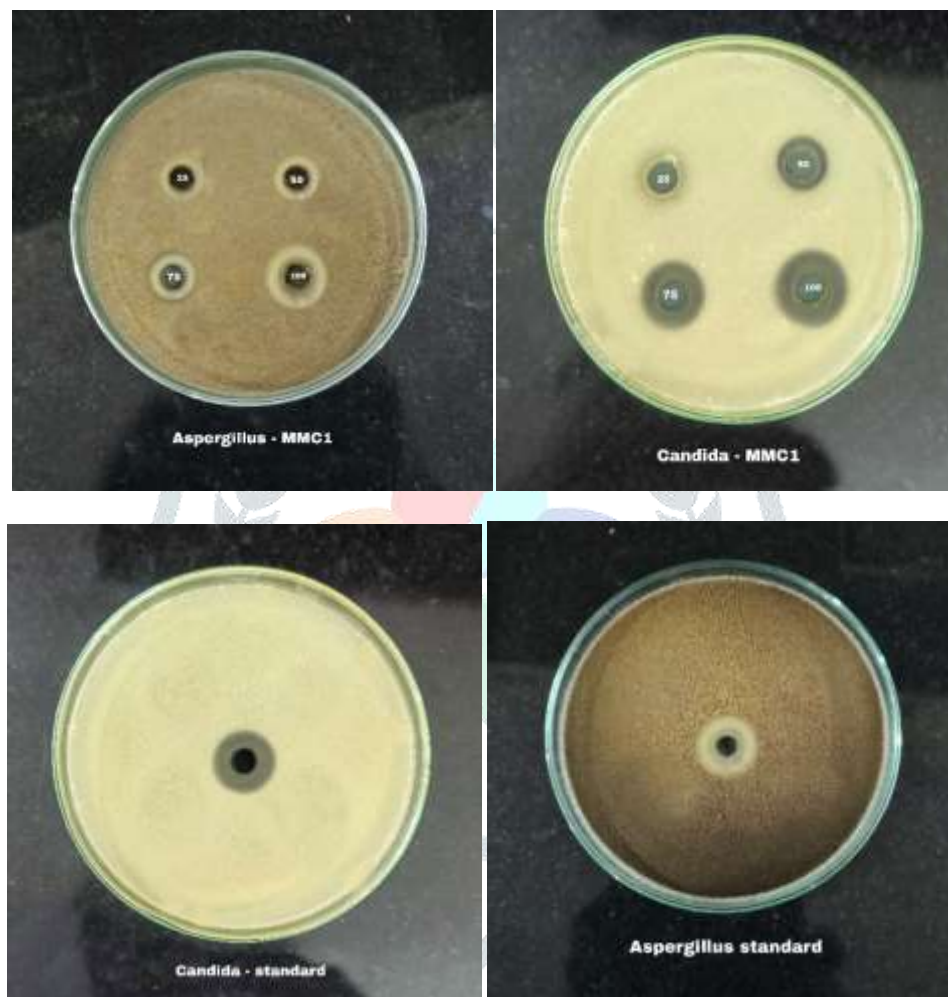


Fig.16. Antifungal activity of $[\text{Ru}(\text{phen})_2(\text{MTPIP})]^{+2}$ Complex

3.4. Cytotoxicity

The MTT method was used to evaluate the antiproliferative activities of the Ru(II) Complexes against MCF-7 (Human breast cancer), comparison with doxorubicin as positive control. The Ru(II) polypyridyl complex displays excellent antitumour activity towards the selected cancer cell line. Ru(II) complex exhibited well activity against MCF-7 cells with $\text{IC}_{50} = 14.54 \pm 0.19 \mu\text{g/ml}$ and standard doxorubicin $\text{IC}_{50} = 3.66 \pm 0.07 \mu\text{g/ml}$. Cell viability of MCF-7 is more in case of complex because of the presence of phenanthroline ligand shown in the figure 17. Thus this complex exhibits high inhibitory effect on the cell growth in MCF-7 cell line and may be used as a potent anticancer drug against breast cancer.

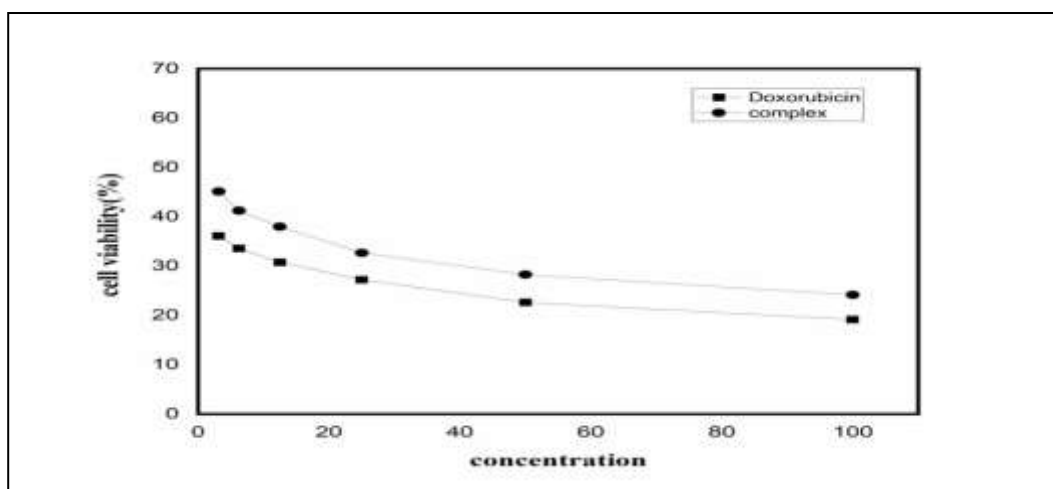


Fig. 17. Cell viability of MCF-7 cell line in vitro treatment with complexes $[\text{Ru}(\text{phen})_2(\text{MTPIP})]^{+2}$. Every data point is the average \pm standard error derived from a minimum of three separate experiments.

4. CONCLUSION

Ru(II) polypyridyl complex are synthesized with novel intercalator MTPIP ligand, characterized and their interaction with CT-DNA was studied by UV-Vis absorption, fluorescence quenching titrations and viscosity measurement which concluded that binding mode of complex with DNA is an intercalative mode. The binding constant K_b from UV-Vis absorption studies is 2.5×10^5 and Stern-Volmer quenching constant (K_{sv}) from fluorescence studies is 5.5×10^3 . The binding constant (K_b) from emission studies is 4.1×10^5 . Upon irradiation, this complex can effectively cleave pBR 322 DNA. Antimicrobial activity indicated that complex was active against the tested microorganisms. The *invitro* cytotoxicity of Ru(II) polypyridyl complex show promising anticancer activity against cell line MCF-7.

Acknowledgement-The authors MN and NN are thankful to the Head, Department of Chemistry and the Principal, University college of Science, Saifabad, Osmania University and The Head, Department of Chemistry and The Principal, University College of Science, Tarnaka, Osmania University, Hyderabad for the facilities to carry out this work. The Authors are thankful to the DST FIST, New Delhi for facility of the Computational Lab at Department of Chemistry, University College of Science Saifabad, Osmania University.

Conflict of Interest-On behalf of all authors, the corresponding author states that there is no conflict of interest.

References

- Dabrowiak JC (2009) Nano medicine. In metals in medicine. Wiley.
- Roat malone Rm(2002) Bio inorganic chemistry a short course Wiley.
- Rasko DA, sperandio V (2010) Anti-virulence strategies to combat bacteria-mediated disease. Nat Rev drug Discov. 9:117-128. <https://doi.org/10.1038/nrd.3013>
- Blair JMA, webber MA, Baylay AJ et al (2015) molecular mechanisms of antibiotic resistance, Nat Rev microbial 13:42-51. <https://doi.org/10.1038/nrmicro.3380>
- Spellberg B, Blasér M, Guidos RJ et al (2011) combating anti microbial resistance; policy Recommendation to save lives. Clin infect DIS 52:53 97-428. <http://doi.org/10.1093/cid/cir153>
- Rosenberg B (1978) Platinum complexes for the treatment of cancer. Interdiscip Sci. Rev 3:134-147
- Werbeck ND, Zeymw C, Kellner JN, Rein stein J (2011) coupling of oligomerization and nucleotide binding in the AAA⁺ chaperone clp B. Bio chemistry 50: 899-909
- Yu Hy, Zhang S, Dunn MR, Chatput JC (2013) An efficient and faithful in vitro replication system for threous nucleic acid. J Am chem. SOC 135:3583-3591
- Chen W, Schuster GB (2013) Precise sequence control in linear and cyclic copolymers of 2,5-Bis(2-thienyl)pyrroie and aniline by DNA-Programmed assembly, j Am chem soc 135:4438-4449
- World Health Organization, Antimicrobial resistance (2018) october 13, 2019, <http://www.who.int/news-room/factsheets/detail/antimicrobial-resistance>. Accessed 13 Sept 2021
- Antimicrobial resistance is rising in India-says- icmr-report/article show/85913195. Cms. Accessed 14 Sept 2021
- K.J. Herbst, M.D Allen, J.Zhang, J. Am. Chem. Soc. 2011, 133, 5676-5679
- R.S. Sanchez, R. Gras-Charles, J.L. Bourdelande, G. Guirado, J. Hernando, J. Phys. Chem. c 2012, 116, 7164-7172.
- A Praetorius D.M. Baily, T Schwarzlose W.M. Nau .org.lett 2008, 10 4089-4092
- C. Zhoy, .Y. Li. Y. Zhao, J. Zhang, W. yang, W. Yang, W. Yang y. Li .org.lett. 2011, 13 292-295
- A. S. Stepanov, V.V. Yanilkin, A.R. Mustafina, V.A. Buriilov, S.S. Solovieva, I. Antipin, A.I. Konovalov, Electrochem. Commun. 2010, 12, 703-705.
- Q.M. Wang, K. Ogawa, K. Toma, H. Tamiaki J. Photochem. Photobiol. A 2009, 201, 87-90

18. T. Ayers, N. Caylar, G. Ayers, C. Godwin, D. J. Hathcock, V. Stuman, S. J. Slattery, In *org. chim. Acta* 2002, 328, 33-38.
19. S. H. Fan, A. G. Zhang, C. C. Ju, L. H. Gao, K. Z. Wang. In *Org. chem.* 2010, 49, 3752-3763
20. F. Gao, X. Chen, F. Zhou, L. P. Weng, L. T. Guo, M. Chen, L. N. Ji. In *org chim. Acta* 2011, 370, 132-140
21. Rosenberg B (1978) Platinum complexes for the treatment of cancer *Interdiscip sci Rev* 3:134-147
22. Furetes MA, Alonso C, Perez JM (2003) Biochemical modulation of cisplatin mechanisms of action: enhancement of anti tumour activity and circumvention of drug resistance. *Chem Rev* 103:645-662
23. Akiyama S, Chen ZS, Sumizawa T, Furukawa T (1999) Resistance to cisplatin. *Anti cancer drug Des* 14:143-151
24. Milacic V, Dou QP (2009) The tumor proteasome as a novel target for gold (III) complexes: implications for breast cancer therapy. *Coord chem. Rev* 253:1649-1660
25. Quiroga AG, Ranninger CN (2004) Contribution to the SAR field of metallated and coordination complexes studies of the palladium and platinum derivatives with selected thiosemicarbazones as anti tumoral drugs *Coord chem. Rev* 248:119-133.
26. Pellerito L, Nagy L (2002) organotin(IV) N⁺ complexes formed with biologically active ligands equilibrium and structural studies and some biological aspects. *Coord chem. Rev* 224:111-150
27. Jain SS, Anderson CM, Dirienzo F, Taylor IR, Jain K, Guha S, Hoque N (2013) RNA binding and inhibition of primer extension by a Ru(III)/Pt(II) Metal complex *Chem. Commun* 49:5031-5033.
28. Anderson CM, Taylor IR, Tibbetts MF, Philpott J, Hu Y, Tanski JM (2012) Hetero-multi nuclear ruthenium(III)/Platinum(II) complex that potentially exhibit both antimetastatic and antineoplastic properties. In *org chem* 51:12917-12924.
29. Auzias M, Gueniat J, Therrien B, Sussfink G, Renfrew AK, Dyson PJ (2009) Arene ruthenium complex with ferrocene derived ligands; synthesis and characterization of complexes of the type [Ru(η^6 -arene)(NC₅H₄CH₂NHOC-C₅H₄FeC₅H₅)Cl₂] and [Ru(η^6 -arene)(NC₃H₃(CH₂)₂O₂C-C₅H₄FeC₅H₅)Cl₂] *J Organomet chem.* 694:855-861
30. Rajaraman A, Sahoo AR, Hildfischmeister C, Achard M, Bruneau C (2015) *Datton Trans* 44(40):17467-17472.
31. Comba P (2021), modeling of molecular properties in comprehensive coordination chemistry 3 Comba (ed) Elsevier, Wiley-VCH 107-121
32. Antonarakis ES, Emadi A (2010) *cancer chemother pharmacol* 66(I) 1-9
33. Araya G, Benites J, Reyes JS, Marcoleta AE, Valderrama JA, Lagos R, Monasterio (2019) Inhibition of Escherichia coli and Bacillus subtilis FtsZ polymerization and bacillus subtilis growth by dihydroxynaphthyl aryl ketones. *Front microbial* 10:1225 <https://doi-org/10.3389/fmicb.2019.01225>.
34. M. Yamada, Y. Tanaka, Y. Yoshimoto, S. Kuroda, I. Shima. *Bull. Chem. Soc. Jpn.*, **1992**, 65, 1006. <https://doi.org/10.1246/bcsj.65.1006>
35. B.P. Sullivan, D.J. Salmon, T. Meyer. *Inorg. Chem.*, 17, 3334 (1978). <https://doi.org/10.1021/ic50190a006>
36. Sravani Gudikandula, Navaneetha Nambigari. Correlation of Anti-cancer activity and DNA binding affinity of novel Ru(II) Polypyridyl complex – A Biophysical study, 2024 *J. Emer Trends in ETIR* February 2024, Volume 11, Issue 2 www.jetir.org (ISSN-2349-5162)
37. N. Navaneetha, K. Aruna, V. Ravi Kumar, A. Praveen Kumar, S. Satyanarayana, A Biophysical Study of Ru(II) Polypyridyl Complex, Properties and its Interaction with DNA. *Journal of Fluorescence*. **2022**, 32(3):1211-1228 <https://doi.org/10.1007/s10895-021-02879-x>
38. N. Navaneetha, K. Aruna, V. Ravi Kumar, A. Praveen Kumar, S. Satyanarayana, Binding and Photocleavage studies of Ru (II) Polypyridyl Complexes with DNA: An In Silico and Antibacterial activity. *Analytical Chemistry Letters*. **2022**. 12 (2), 266 – 282. <http://doi.org/10.1080/22297928.20211110>.
39. S. Satyanarayana, J.C. Dabrowiak, J.B. Chaires. *Biochem.*, 32, 2573 (1993).
40. Lakowicz, J. R.; Weber, G. Quenching of Fluorescence by Oxygen. A Probe for Structural Fluctuations in Macromolecules. *Biochemistry*. 1973, 12, 4161–4170. <https://doi.org/10.1021/bi00745a020>
41. Lakowicz, J. R.; Weber, G. Quenching of Fluorescence by Oxygen. A Probe for Structural Fluctuations in Macromolecules. *Biochemistry*. 1973, 12, 4161–4170. <https://doi.org/10.1021/bi00745a020>
42. Vuradi, Ravi Kumar | Nambigari, Navaneetha | Pendyala, Pushpanjali | Gopu, Srinivas | Kotha, Laxma Reddy | G, Deepika | M, Vinoda Rani | Sirasani, Satyanarayana. Study of Anti-Apoptotic mechanism of Ruthenium (II) Polypyridyl Complexes via RT-PCR and DNA binding. *App. Organomet. Chem*, 34(3) (2020). [10.1002/aoc.5332](https://doi.org/10.1002/aoc.5332).
43. Satyanarayana S, Dabrowiak JC, Chaires JB (1993) Tris (phenanthroline) ruthenium (II) enantiomer interactions with DNA: mode and specificity of binding. *Biochemistry*, 32(10), 2573-2584. [doi: 10.1021/bi00061a015](https://doi.org/10.1021/bi00061a015).